Nonlinear Modeling of Super-Resolution Near Field Structure System based on the Volterra and Neural Network Models

Manjung Seo and Sungbin Im
School of Electronic Engineering, Soongsil University
511 Sangdo-dong, Dongjak-gu, Seoul 156-743, Korea
E-mail: baoro33@ssu.ac.kr, sbi@ssu.ac.kr

Abstract: Reliable channel modeling becomes an important measure in performance evaluation on various data detection algorithms. For this reason, correct and accurate modeling is required. This paper presents a nonlinear modeling of Super-RENS (Super-Resolution Near Field Structure) read-out signal using the second-order Volterra and neural network models. The experiment results verified the possibility that Volterra and neural network models can be utilized for nonlinear modeling of Super-RENS systems. Furthermore, nonlinear equalizers can be developed based on the information obtained from this nonlinear modeling.

1. Introduction

Recently, various recording technologies are investigated for optical data storage. Upon completing the standardization of BD (Blu-ray Disc) and High-Definition Digital Versatile Disc (HD-DVD), the industry is looking for a suitable technology for the next generation optical data storage. In general, diffraction ultimately limits the maximum data density of conventional optical data storage devices. The density is proportional to the ratio NA/λ, where λ is the wavelength of the laser source and NA is the numerical aperture of the playback optical system. One way to exceed this limit is to use a super resolving imaging technique. For example, a very small aperture (VSAL)[1] or a solid immersion lens (SIL)[2] can be used to read very small (sub-diffraction limit sized) data marks on the disc. These techniques use evanescent coupling of a very small spot of external laser light from the playback head into the data surface of the disc. The third technique, which has been proposed as a method of exceeding the density restriction imposed by the diffraction limit, is Super-resolution near field structure (Super-RENS).[3-6]

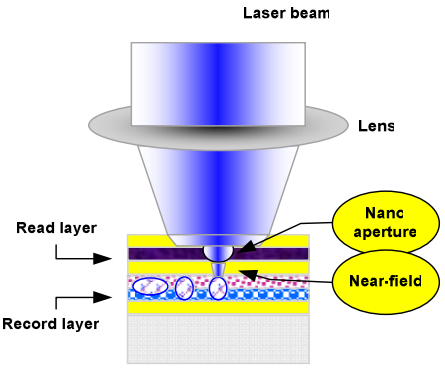

Figure 1. Structure of the Super-RENS disc.

By comparing various approaches, it has gradually turned out that the technique that uses the Super-RENS disc is the most promising one for the next generation optical data storage system to succeed BD, due to its compatibility with and easy replacement of the existing systems. The Super-RENS disc enables to read pits smaller than the optical resolution limit by employing an optically nonlinear effect generated in phase change (PC) media. Several researchers achieved higher capacities over 100 GB using various types of Super-RENS discs. The carrier-to-noise ratio (CNR) now exceeds 40 dB for 37.5 nm recording pits. The disc enables four times larger capacity than the BD only along the tangential direction of the recording track. Furthermore, a dual-layer type of super-resolution layers was reported to increase the capacity twofold.

In this paper, we apply the Volterra[7,8] model and neural networks for nonlinear modeling of Super-RENS system. The approaches based on Volterra filters have a firm mathematical foundation and can describe a broad class of nonlinear phenomena. Furthermore, since the output of a Volterra filter depends linearly on the linear and quadratic filter coefficients (but nonlinearly on the input), many concepts originally developed for linear filters can be extended to Volterra filters. Moreover, through the use of Volterra filters to model nonlinear systems, one often gains new insight into the physical mechanisms underlying such nonlinear systems[9]. The model structure of neural networks considered in this paper is the NARX (Nonlinear AutoRegressive eXogenous)[10] model. In this paper, we compared modeling performance of neural network with the Volterra model.

This paper is organized as follows. In Sections 2, and 3 the Volterra model and the NARX model are introduced, respectively. The simulation results are presented in Section 4. Finally, the paper is concluded in Section 5.

2. The Volterra Model

In general, we assume that the nonlinear system to be represented by a Volterra filter is stable and has finite memory. The Volterra series[7] can approximate the output of the nonlinear system by its sampled data form the output of which can be represented as

$$\begin{aligned} Y(k) = & \sum_{\tau_1=0}^{N-1} h_1(\tau_1) X(k-\tau_1) \\ & + \sum_{\tau_1=0}^{N-1}\sum_{\tau_2=0}^{N-1} h_2(\tau_1,\tau_2) X(k-\tau_1) X(k-\tau_2) \\ & + \sum_{\tau_1=0}^{N-1}\sum_{\tau_2=0}^{N-1}\sum_{\tau_3=0}^{N-1} h_3(\tau_1,\tau_2,\tau_3) X(k-\tau_1) X(k-\tau_2) X(k-\tau_3) \\ & + \cdots \end{aligned} \tag{1}$$

where $X(k)$ denotes the input sequence to the system, $Y(k)$ denotes the system output sequence predicted by the Volterra filter, and $h_1(\tau_1)$, $h_2(\tau_1,\tau_2)$, $h_3(\tau_1,\tau_2,\tau_3)$ represent the linear, quadratic, and cubic Volterra coefficients, respectively. Since the Volterra filter can be interpreted as a generalized Taylor series representation of a function with memory, the Volterra filter can be interpreted as an extension of a linear filter in that a quadratic filter, a cubic filter, and so on, are appended in parallel to a linear filter. For this reason, Volterra filters can describe a broad class of gently nonlinear systems.

3. The NARX Model

The NARX model is a recurrent dynamic network, where feedback connections can enclose several layers of the network. Since it is based on the linear ARX model, which is commonly used in time series modeling, it has many desirable features. The structure of the NARX model is shown in Figure 2.

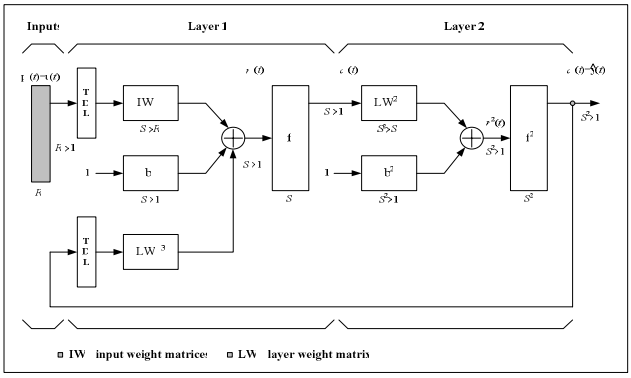

Figure 2. Structure of the NARX model.

The NARX model consists of two layers; a feed-forward network with a tapped delay line at the input and an output layer. As shown in Figure 3, the function of Layer 1, f^1, employs the tangent sigmoid function while that of Layer 2, f^2, is the purely linear function.

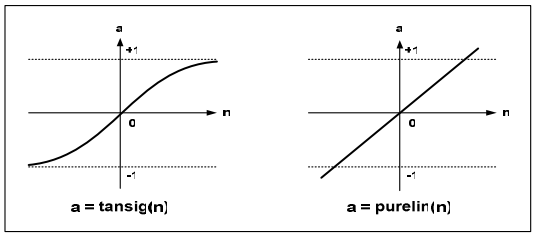

Figure 3. Transfer function of the NARX model.

The defining equation for the NARX model is

$$y(t) = f(y(t-1), y(t-2), \ldots, y(t-n_y), \\ u(t-1), u(t-2), \ldots, u(t-n_u)) \quad (2)$$

where $y(t)$ and $u(t)$ represent the model output and input, respectively. The parameters n_y and n_u are the orders of the TDL (Tapped Delay Lines) for output and input, respectively. The parameters of the NARX model are summarized in Table 1.

Table 1. Parameters of the NARX model.

R	Number of elements in input vector
S	Number of neurons in layer
p	Input vector
W	Weight matrix
n	S-element net input vector scalar output
a	The neuron layer outputs form a column vector
b	Bias vector
f	Transfer function

4. Experiment and Results

The physical conditions of obtaining the Super-RENS signal samples used in the experiments are as follows. The minimum mark size is 150 nm, the linear velocity of the disk is 4.92 m/s, the wavelength is 405 nm, and the NA (numerical aperture) is 0.85. Those are summarized in Table 2 and more details of the disk properties can be found in ref [11]. Figure 4 shows the block diagram of the experiment setups in this work. We pre-process the RF signal in order to make more efficient modeling. In the pre-processing block, the target signal, that is, RF signal, is filtered to remove low frequency noise using a high-pass filter of stop band from DC to 2.5 MHz. The DC component and the low frequency noise are located outside the information band because the lowest information frequency is 4.125 MHz for 8T signal.

Table 2. Summary of the disc properties.

Disc	BD (Blu-ray)
Recording layer	Metal/Si
Diameter (cm)	12
Cover (mm)	0.1
Track pitch (nm)	320
Laser wavelength (nm)	405
Minimum mark size (nm)	150
Linear velocity (m/s)	4.92
NA	0.85
Dynamic tester	Pulstec ODU-1000
Recording power (mW)	9.3
Readout power (mW)	1.2

Figure 5 shows MSE (Mean Square Error) curves according to the delay ranges of the Volterra filter. The MSE is measured by

$$MSE = \frac{1}{Q}\sum_{k=1}^{Q} e(k)^2 = \frac{1}{Q}\sum_{k=1}^{Q} (d(k) - y(k))^2 \quad (3)$$

where $d(k)$ denotes the original RF signal, $y(k)$ denotes the system output signal by the Volterra filter, and $e(k)$ represents the error between $d(k)$ and $y(k)$.

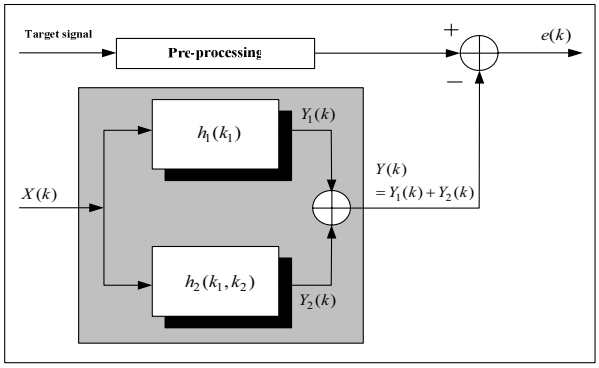

(a) Volterra Model

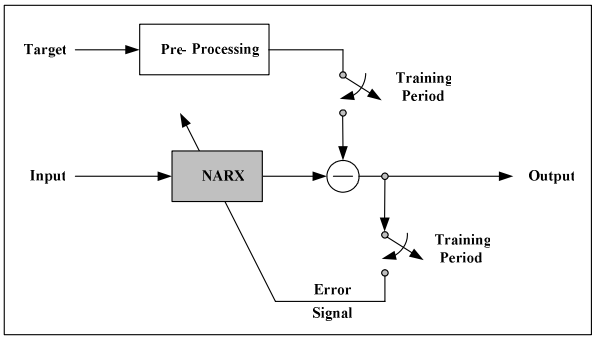

(b) NARX Model

Figure 4. Block diagram of the experiment setup.

Table 3. MSE's according to the input delay ranges of the NARX model.

Number of neuron	Input delay ranges	MSE
5	0～3	0.0155
	0～6	0.0085
	0～10	0.0065
	⋮	⋮
	0～25	0.0055

Figure 6 shows a part of the estimated and original waveforms of Super-RENS RF signal to demonstrate the nonlinear modeling performance of the Volterra model. The experiment results reveal that the MSE of the Volterra model output signal with respect to the original RF signal is about 1.6×10^{-3}. Figure 7 depicts the MSE curves of the NARX model for various training algorithms. As shown in Figure 7, the Levenberg-Marquardt algorithm[12] achieves the minimum MSE. In Table 3, using this training algorithm, the MSE's of the NARX model are listed according to the input delay ranges from 3 to 25 with the output delay range from 1 to 2 in Layer 1. Layer 1 consists of 5 neurons while Layer 2 uses one neuron. As observed in Table 3, as the input delay range increases, the MSE decreases, but the number of weights increases. In this experiment, we chose the input delay range from 0 to 10. The MSE of NARX output signal with respect to the original RF signal is about 6.5×10^{-3}.

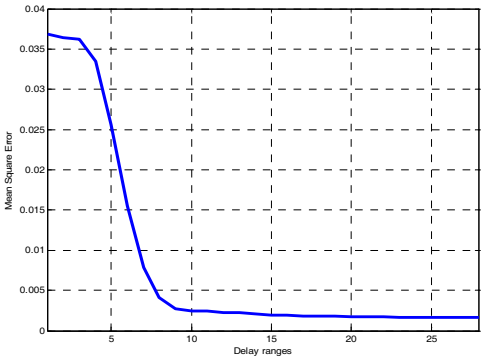

Figure 5. MSE's vs. delay ranges of the Volterra filter.

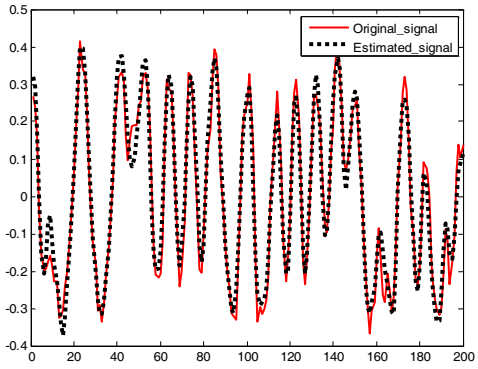

Figure 6. RF signal vs. Volterra filter output signal.

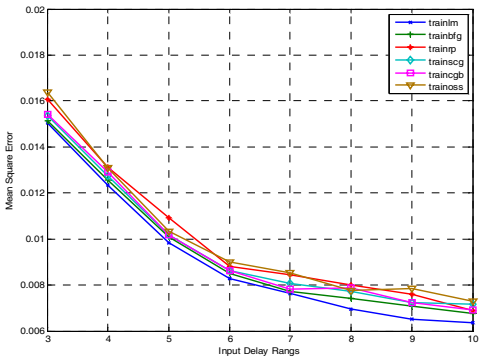

Figure 7. MSE's vs. input delay ranges for various training algorithm.

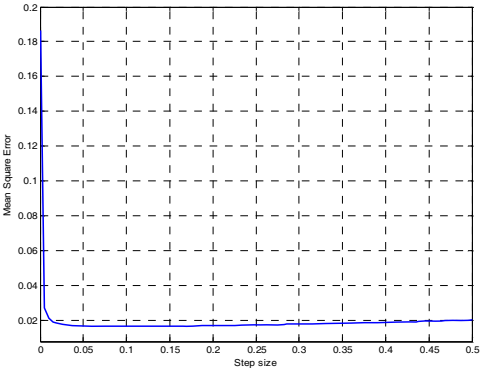

Figure 8. MSE's for various step sizes of the NLMS FIR filter.

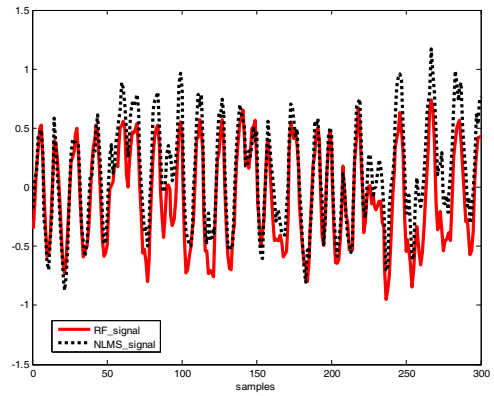

Figure 9. Comparison of the RF signal and the FIR filter output signal.

For the purpose of comparison, we performed FIR (Finite Impulse Response) linear modeling with NLMS (Normalized Least Mean Square). Figure 8 shows the MSE curve for various step sizes of the NLMS FIR filter, where the number of filter taps is set to 76 and step size varies from 0 to 0.5. The minimum MSE is 1.65×10^{-2} when the step size is 0.09. Figure 9 shows a part of the waveforms of the RF signal and the FIR filter output signal. The experiment results demonstrate that the linear modeling based on the FIR filter is not appropriate to modeling the Super-RENS disc system because of its limited performance.[13]

5. Conclusion

This paper presents the results of applying the Volterra model and the neural networks to nonlinear modeling of the Super-RENS system. According to the experiment results, the MSE's between the RF signal and the output signals of the second-order Volterra and the neural network models are less than that between the RF signal and the output signal of the NLMS FIR adaptive filter, which is one of linear modeling approaches. This implies that the Volterra model and the neural networks are more suitable for modeling of Super-RENS systems.

References

[1] A. Partovi, D. Peale D, M.Wutting, C. A. Murray, G. Zydzik, L. Hopkins, K. Baldwin, W. S. Hobson, J. Wynn, G. Lopata, L. Dhar, R. Chichester, and J. H-J Yeh, "High-power laser light source for near-field optics and its application to high-density optical data storage," *Appl. Phys. Lett.*, vol. 75, no. 11, pp. 1515-1517, Sep. 1999.

[2] E. Betzig, J. K. Trautman, R. Wolfe, E. M. Gyorgy, P. L. Finn, M. H. Kryder, and C. H. Chang, "Near-field magneto-optics and high density data storage," *Appl. Phys. Lett.*, vol. 61, no. 2, pp. 142-144, Jul. 1992.

[3] J. Tominaga, T. Nakano, and N. Atoda, "An approach for recording and readout beyond the diffraction limit with an Sb thin film," *Appl. Phys. Lett.*, vol. 73, no. 15, pp. 2078-2080, Oct. 1998.

[4] T. Nakano, A. Sato, H. Fuji, J. Tominaga, and N. Atoda, "Transmitted signal detection of optical disks with a superresolution near-field structure," *Appl. Phys. Lett.*, vol. 75, no. 2, pp. 151-153, Jul. 1999.

[5] D. P. Tsai and W. C. Lin, "Probing the near fields of the super-resolution near-field optical structure," Appl. *Phys. Lett.*, vol. 77, no. 10, pp. 1413-1415, Sep. 2000.

[6] T. Kikukawa, T. Nakano, T. Shima, and J. Tominaga, "Rigid bubble pit formation and huge signal enhancement in super-resolution near-field structure disk with platinum-oxide layer," *Appl. Phys. Lett.*, vol. 81, no. 25, pp. 4697-4699, Dec. 2002.

[7] M. Schetzen, *The Volterra and Wiener Theories of Nonlinear Systems*, New York: Wiley, 1980.

[8] S. Im and E. J. Powers, "A Fast Method of Discrete Third-Order Volterra Filtering," *IEEE Trans. on Signal Processing*, vol. 44, no. 9, pp. 2195-2208, Sep. 1996.

[9] C. P. Ritz, E. J. Powers, and R. D. Bengtson, "Experimental measurement of three-wave coupling and energy cascading," *Phys. Fluids*, vol. B1, pp. 153-163, Jan. 1989.

[10] Feng, J., C.K. Tse, and F.C.M. Lau, "A neural-network-based channel-equalization strategy for chaos-based communication systems," *IEEE Trans. on Circuits and Systems I: Fundamental Theory and Applications*, vol. 50, no. 7, pp. 954–957, 2003.

[11] K. Kwak, S. Kim, C. Lee, and K. Song, "New materials for super-resolution disc," *SPIE Proceedings*, vol. 6620, ODS2007 TuC5, 2007.

[12] Hagan, M,T., and M.Menhaj, "Training feed-forward networks with the Marquardt algorithm," *IEEE Trans. on Neural Networks*, vol. 5, no. 6, pp. 989-993, 1999.

[13] Manjung Seo, Sungbin Im, and Jaejin Lee, "Nonlinear Modeling of Super-RENS System Using a Neural Networks," *IEEK TeleCommun.*, vol/ 45-TC, no. 3, pp. 53-60, Mar. 2008.